

1
2
3
4
5
6
7
8
9
10
11
12
13
14
15
16
17
18
19
20

Exploring the use of SEM-EDS analysis to measure the distribution of major, minor, and trace elements in bottlenose dolphin (*Tursiops truncatus*) teeth

Meaghan A. McCormack^{a*}, Wayne E. McFee^b, Heidi R. Whitehead^c, Sarah Piwetz^c, and Jessica Dutton^a

^aDepartment of Biology, Texas State University, Aquatic Station, San Marcos, TX 78666, USA

^bNational Centers for Coastal Ocean Science, National Oceanic and Atmospheric Administration, Charleston, SC 29412, USA

^cTexas Marine Mammal Stranding Network, Galveston, TX 77551, USA

Corresponding author

Meaghan McCormack
Department of Biology, Texas State University, Aquatic Station, San Marcos, TX 78666, USA
mmccormack@txstate.edu
ORCID ID: 0000-0001-6623-3892

21 **Acknowledgments**

22 We would like to express our gratitude to the Analysis Research Service Center (ARSC) at
23 Texas State University, especially Jonathan Anderson and Brian Samuels, for training and use of
24 the SEM-EDS. The ARSC JEOL SEM equipment purchase was made possible by Professor Tom
25 Myers (startup funds), Emerging Technology Fund (grant), MSEC, Provost, and Research
26 Service Center contributions. Teeth were provided by the Texas Marine Mammal Stranding
27 Network under a NOAA parts authorization letter pursuant to 50 CFR 216.22. issued to Jessica
28 Dutton. NOAA Disclaimer: The scientific results and conclusions, as well as any opinions
29 expressed herein, are those of the authors and do not necessarily reflect the views of NOAA or
30 the Department of Commerce. The mention of any commercial product is not meant as an
31 endorsement by the Agency or Department.

32

33

34

35

36

37

38

39

40

41

42 **Abstract**

43 Dolphin teeth contain enamel, dentin, and cementum. In dentin, growth layer groups (GLG's),
44 deposited at incremental rates (e.g., annually), are used for aging. Major, minor, and trace
45 elements are incorporated within teeth; their distribution within teeth varies, reflecting tooth
46 function and temporal changes in an individual's exposure. This study used a scanning electron
47 microscope (SEM) equipped with energy dispersive X-ray spectroscopy (EDS) to determine the
48 distribution of major (e.g., Ca, P), minor (e.g., Cl, Mg, Na), and trace elements (e.g., Cd, Hg, Pb,
49 Zn) in teeth from 12 bottlenose dolphins (*Tursiops truncatus*). The objective was to compare
50 elemental distributions between enamel and dentin and across GLG's. Across all dolphins and
51 point analyses, the following elements were detected in descending weight percentage (wt %;
52 mean \pm SE): O (40.8 ± 0.236), Ca (24.3 ± 0.182), C (14.3 ± 0.409) P (14.0 ± 0.095), Al ($4.28 \pm$
53 0.295), Mg (1.89 ± 0.047), Na (0.666 ± 0.008), Cl (0.083 ± 0.003). Chlorine and Mg differed
54 between enamel and dentin; Mg increased from the enamel towards the dentin while Cl
55 decreased. The wt % of elements did not vary significantly across the approximate location of
56 the GLG's. Except for Al, which may be due to backscatter from the SEM stub, we did not detect
57 trace elements. Other trace elements, if present, are below the detection limit. Technologies with
58 lower detection limits [e.g., laser ablation inductively coupled plasma mass spectrometry (LA-
59 ICP-MS)] would be required to confirm the presence and distribution of trace elements in
60 bottlenose dolphin teeth.

61 **Keywords**

62 Elemental microanalysis; Scanning electron microscopy; Energy dispersive x-ray spectroscopy;
63 Bottlenose dolphin; Enamel; Dentin

64 **Declarations**

65 **Funding**

66 Funding for this project was provided by the Texas State University Graduate College Doctoral
67 Research Support Fellowship to Meaghan McCormack.

68 **Conflict of interest/Competing interests**

69 The authors have no conflicting or competing interests to declare.

70 **Availability of data and material**

71 Data for each dolphin is available in the supplementary information. Any data and images not
72 published in this paper can be requested from Meaghan McCormack at
73 mmccormack@txstate.edu.

74 **Code availability**

75 Not applicable

76 **Author's contributions**

77 Meaghan A. McCormack: Conceptualization, Data curation, Formal analysis, Funding
78 acquisition, Methodology, Writing - original draft, Writing – review & editing. Wayne E.
79 McFee: Data curation, Methodology, Formal analysis, Writing - review & editing. Heidi R.
80 Whitehead: Sample acquisition, Writing – original draft, Writing - review & editing. Sarah

81 Piwetz: Sample acquisition, Writing – original draft, Writing - review & editing. Jessica Dutton:
82 Conceptualization, Supervision, Writing – original, draft, Writing - review & editing.

83

84 **1. Introduction**

85 Dolphins have evolved homodont dentition; their simplified cone shaped teeth are also
86 greater in number compared to terrestrial mammals [1-4]. The evolution of dolphin dentition is
87 likely a consequence of their foraging behavior and the absence of mastication [2]. Further, in
88 contrast to most terrestrial mammals, which are diphyodonts and produce two sets of teeth
89 (deciduous and permanent), dolphins are monophyodonts and develop only one set of teeth [1, 5-
90 6]. In marine mammals, teeth grow incrementally, and once incorporated within the tooth
91 structure, major [e.g., calcium (C), phosphorous (P)], minor [e.g., chlorine (Cl) magnesium (Mg),
92 sodium (Na)], and trace elements [e.g., cadmium (Cd), mercury (Hg), lead (Pb), zinc (Zn)]
93 remain unaltered, thereby reflecting an organism’s physiology, ambient environmental
94 conditions, dietary intake, and exposure to trace elements including contaminants [e.g., Cd,
95 chromium (Cr), Pb, Hg] [7-17]. The chemical composition of teeth and the spatial distribution of
96 major and minor elements within teeth influences tooth function [18-19]. For example, in human
97 teeth, a decrease in tooth hardness has been associated with increases in the weight percentage
98 (wt %) of Na₂O and MgO and decreases in the wt % of P₂O₅ and CaO [20]. Additionally, the
99 pattern of trace element deposition within dolphin teeth may reflect the maternal transfer of
100 contaminants, the timing of life-history events [e.g., Zn to estimate age at maturity], and habitat
101 use [e.g., barium (Ba) as a proxy for salinity] [8, 10, 15].

102 Like other mammalian teeth, dolphin teeth consist of three primary components: enamel,
103 dentin, and cementum [1, 3-5, 19]. Structurally, the tooth consists of nested layers. On the
104 exterior, the enamel and cementum line the tooth crown and root, respectively. Following the
105 enamel and cementum is the dentin, which surrounds the central pulp cavity [21]. Development
106 of the enamel and dentin begins while the dolphin is *in utero*, while cementum begins developing
107 after birth [1]. In dolphins, dentin layers accumulate along the edges of the pulp cavity at
108 predictable rates (e.g., annually), slowly decreasing the volume of the pulp cavity; collectively,
109 the layers of dentin are referred to as growth layer groups (GLG's) [21-24].

110 Enamel, dentin, and cementum are comprised of water, inorganic components, primarily
111 hydroxyapatite [$\text{Ca}_{10}(\text{PO}_4)_6(\text{OH})_2$], and organic components (e.g., proteins) [18-19, 25-26].
112 Although these three dental tissues have a similar mineral composition, the proportion of
113 inorganic and organic materials varies among the tissues; notably, the enamel is the hardest of the
114 tissues, comprised of 95-96% inorganic material, while the dentin and cementum are softer
115 tissues comprised of a lower percentage of inorganic material (e.g., 70% inorganic material in
116 dentin) [27-29]. Calcium and P are the main components of hydroxyapatite and, as a result, are
117 the major elements present in teeth. The structure of hydroxyapatite includes several cationic and
118 anionic sites; therefore, a variety of minor and trace elements can be incorporated within its
119 chemical structure [30-31]. For example, cations such as Cu^{2+} , K^+ , Mg^{2+} , Na^+ , Ni^{2+} , Pb^{2+} , or Zn^{2+}
120 may substitute for Ca^{2+} , while anions such as CO_3^{2-} and SiO_4^{4-} , or Cl^- and F^- may replace PO_4^{3-}
121 and OH^- , respectively [30-36]. In addition to being incorporated within the mineral structure
122 itself, elements (e.g., Zn) associated with macromolecules on the surface of the crystalline lattice
123 may become trapped as new mineral layers are deposited [37]. In marine mammals, more than
124 20 elements have been reported in dental tissues including Ba, carbon (C), Ca, Cd, Cl, copper

125 (Cu), Cr, cobalt (Co), fluorine (F), iron (Fe), Pb, Mg, Hg, P, selenium (Se), Na, strontium (Sr),
126 vanadium (V), and Z [8-13, 15,17, 19, 38-41]

127 To determine the elemental composition within the tooth structure, several *in situ* analytical
128 methods are currently available. Some techniques involve the use of electron or proton
129 microprobes with X-ray emission detectors, such as scanning electron microscopes (SEM)
130 equipped with energy dispersive X-ray detection (EDS) and particle-induced X-ray fluorescence
131 (PIXE), respectively [19, 38, 40-41]. These techniques are advantageous because they require
132 little sample preparation and have the spatial resolution necessary to measure the concentration
133 or wt % of elements within GLG's. Further, for studies with methodologies that do not require
134 tooth sectioning or studies that utilize teeth that have been previously sectioned, the methods are
135 non-destructive. However, they often lack the sensitivity to detect elements present at low
136 concentrations, although technologies have improved and detection limits can be optimized with
137 proper sample preparation and analytical settings [26, 42-44]. An alternative approach combines
138 the use of laser ablation and inductively coupled plasma mass spectrometry (LA-ICP-MS),
139 which allows for fine-scale spatial resolution (e.g., tens of microns) and high levels of sensitivity
140 (< 1 ppm) but is destructive as it requires ablating the surface of the sample [42-43].

141 In this study, we used SEM-EDS analysis to explore the distribution of major, minor, and
142 trace elements within teeth from twelve bottlenose dolphins (*Tursiops truncatus*) that stranded
143 along the northern Texas coast in Galveston County between 1987 and 2014. The primary
144 objectives were to explore whether the distribution of major, minor, and trace elements in
145 dolphin teeth 1) differed between the enamel and dentin and 2) varied across the dentin GLG's
146 within individuals, which may reflect physiological changes and exposure to major, minor, and
147 trace elements over time. Finally, although our sample size was limited, we sought to

148 qualitatively assess multi-decadal temporal trends in the wt % of trace elements, particularly
149 those of anthropogenic origin (e.g., Cd, Hg, Pb).

150

151 **2. Methods**

152 *2.1. Teeth collection and preservation*

153 We analyzed teeth from six male and six female bottlenose dolphins that stranded
154 between 1987 and 2014 in Galveston County, TX (Table 1). We preferentially chose individuals
155 with straight-line body lengths between 221 cm and 245 cm. In doing so, we aimed to study
156 dolphins that were at least five years old so we could analyze dolphins that had several GLG's
157 but had not yet reached their asymptotic body length [45]. In older dolphins, GLG's become
158 increasingly irregular and can be challenging to decipher [21]. Furthermore, in some cases, the
159 pulp cavity may become occluded. If this occurs, dentin layers no longer accumulate; therefore,
160 if a dolphin lived beyond the time of pulp occlusion, a complete dentin record would not be
161 available [1, 21].

162 Teeth were extracted from the left mandible of dead stranded bottlenose dolphins using
163 an elevator to loosen the gum and connective tissue, and for most dolphins, an extractor was used
164 to lift the tooth free. For most samples, tooth number eight from the proximal end of the
165 mandible and several surrounding teeth were collected. In some cases, a section of the mandible
166 with teeth still intact was cut from the carcass and frozen for subsequent processing and
167 extraction. If teeth were not available from the left mandible, they were extracted from the right
168 mandible. Teeth were either fixed in 10% neutral buffered formalin or stored at -20°C. A large-
169 scale cleaning/preparation project was undertaken in 2017 wherein teeth were removed from

170 formalin prior to preparation. Therefore, some teeth may have been stored in formalin for several
171 decades before 2017; however, no records were kept for which teeth were frozen and which teeth
172 were stored in formalin. In 2017, formalin-fixed teeth were removed from solution and
173 thoroughly rinsed in running tap water. Water maceration was performed on all teeth with
174 attached soft tissue, using separate containers for each dolphin. Any soft tissue that did not
175 detach after soaking was gently brushed away. Teeth were then rinsed and air-dried in a
176 temperature-controlled room and stored in individually labeled Whirl-Pak bags (Nasco; Fort
177 Atkinson, WI) at room temperature. Since a detailed storage history for the teeth was not
178 available, it was not possible to explore the influence of preservation methods on major, minor,
179 and trace elements. Despite disparate storage conditions, we utilized all teeth for both age
180 estimation and SEM-EDS analysis. Formalin preservation may influence tooth elemental
181 composition; however, to the best of our knowledge there have been no studies that investigated
182 the effect of formalin fixation on elemental concentrations in teeth.

183

184 *2.2. Teeth sectioning and age estimation*

185 Teeth were initially sectioned down the center mid-line of the longitudinal buccal-lingual
186 axis. One half of the tooth was used for SEM-EDS analysis, and the other half was prepared for
187 sectioning for age determination using standard procedures [21-22]. Teeth for age determination
188 were fixed in 10% neutral buffered formalin for 48 hours, rinsed in water, and dried before
189 sectioning. Slabs were cut off the longitudinal buccal-lingual axis of each tooth using a diamond
190 wafer blade mounted on a Buehler Isomet low-speed saw (Emerson Industrial Automation, Lake
191 Bluff, IL). The slabs were continuously rinsed in tap water for approximately 6 hours and then

192 decalcified in RDO (rapid decalcifying agent of acids; Apex Engineering Products Corporation,
193 Aurora, IL) for 6-12 hours based on the thickness of the resulting center slab remaining (1-2
194 mm). The slabs were continuously rinsed overnight and thin-sectioned on a Leica SM2000R
195 sledge microtome (Leica, Inc., Nussloch, Germany) attached to a Physitemp freezing stage
196 (Physitemp, Inc., Clifton, New Jersey). Thin sections (25 μm thick) were stained in Mayer's
197 hematoxylin, blued for 30 seconds in a weak ammonia solution, dried on a slide, and mounted in
198 100% glycerin. All sections were read three times by the same reader (Wayne McFee) using a
199 Nikon SMZ1500 stereomicroscope (Nikon Instruments, Inc., Lewisville, Texas); at least one
200 week elapsed between readings to eliminate bias. Teeth were aged based on Hohn et al. [22]; if
201 two of the three readings were the same, this was used as the age estimate, whereas if differences
202 between readings were >2 GLG's, a fourth reading was made. Age estimates >1 GLG were
203 rounded to 0.50 GLG. Most teeth >5 GLG's were estimated to the last GLG.

204

205 *2.3. SEM-EDS analysis*

206 Before SEM-EDS analysis, teeth were rinsed with Milli-Q water (Millipore, Burlington,
207 MA), placed in trace metal clean 50 ml plastic tubes, and ultrasonically cleaned in 95% ethanol
208 for 5 minutes. Teeth were then triple rinsed with Milli-Q water, placed in trace metal clean 15 ml
209 plastic tubes, and air-dried in a clean fume hood for 48 hours. Two analyses on each tooth were
210 performed using an SEM (JSM-6010 PLUS/LA; JEOL USA Inc., Peabody, MA) equipped with
211 EDS at Texas State University. The SEM produces images by scanning the sample with a
212 focused electron beam; the incident electrons interact with the sample, resulting in the production
213 of secondary electrons, backscattered electrons, and characteristic x-rays. Backscattered

214 electrons reflect the composition of the sample, and when examined using an SEM in
215 backscattered electron (BSE) imaging mode, color variation in the sample is indicative of
216 variation in chemical composition [46]. For example, in BSE imaging mode, the enamel, which
217 is more heavily mineralized compared to dentin, appears as a bright band [19, 41]. Characteristic
218 x-rays are generated when the high-energy electron beam ejects an electron from its shell and an
219 electron from a higher energy state transitions to a lower energy state to fill the space. This
220 transition releases characteristic x-rays that are specific to individual elements. Energy dispersive
221 x-ray detectors are often used in conjunction with an SEM to convert characteristic x-rays to
222 electrical voltages to qualitatively and semi-quantitatively describe the distribution of elements
223 in calcified tissues [19, 26, 41-42]. Using SEM-EDS, qualitative and semi-quantitative elemental
224 information at an individual point (point analyses) and across an area (elemental maps) can be
225 obtained, reporting detected elements in wt % or atomic % (at %); when coupled with BSE
226 imagery, one can begin to understand the elemental distribution across the sample.

227 In the first analysis, selective point analysis on three points on the enamel (point 1 = outer
228 enamel, point 2 = mid-enamel, and point 3 = inner enamel) and two points on the pre-natal
229 dentin [point 4 = dentin near the enamel-pre-natal dentin junction (EDJ) and point 5 = inner pre-
230 natal dentin] were performed, following the general methodology outlined by Loch et al. [19] for
231 *in situ* analysis using wavelength dispersive x-ray spectroscopy (WDXS or WDS) (Figure 1).
232 The procedure was repeated for two additional transects, approximately 50 μm apart. Combining
233 the data from the three transects, the mean and standard error (SE) wt % of each element for each
234 point was calculated. A 20 kV accelerating voltage and a working distance of between 10-12 mm
235 was used. In each tooth, point analysis was performed approximately halfway between the tooth

236 neck and the top of the tooth crown. In a subset of teeth ($n = 7$), elemental maps were generated
237 to visualize the distribution of elements across the enamel and pre-natal dentin.

238 In the second analysis, the potential differences in the wt % of elements across the GLG's
239 were explored. Point analysis began halfway between the tooth neck and the bottom of the tooth
240 root. The goal was to obtain measurements from the GLG's; however, GLG's were not visible.
241 Therefore, the approximate location of the GLG's was identified by referencing the images from
242 the thin-crossed sectioned teeth used for aging. Starting from the exterior of the tooth and
243 moving toward the interior, point analyses were performed approximately every 300-350 μm
244 until reaching the pulp cavity (Figure 2). When the pulp cavity was not visible, points were
245 analyzed across half of the tooth width. On average, across all teeth, 7 points per transect were
246 measured; the process was repeated for two more transects approximately 100 μm apart. The
247 mean and SE wt % of the elements detected at each point were calculated. The analytical setting
248 used a 20 kV accelerating voltage, 100 μm aperture size, and a working distance between 9-12
249 mm. Again, for a subset of the samples ($n=2$), elemental maps of the area of interest were
250 generated to qualitatively assess the distribution of elements across the GLG's.

251

252 *2.4. Statistical analysis*

253 For both analyses (enamel vs. dentin and GLG's analysis), a repeated-measures linear
254 mixed effects analysis of variance (ANOVA) and Tukey's post-hoc test was used to explore the
255 potential spatial differences in elemental distribution within the teeth. The repeated-measures
256 design was used because we measured several points on each tooth. In all models, the response
257 variable was the element measured, the fixed effect was the point location [enamel vs. pre-natal

258 dentin (points 1-5) and GLG's analysis (points 1-7)], and the random effect was the individual
259 dolphin (sample). Models with varying intercepts and varying intercepts and slopes were
260 considered, and the model that best fit the data was selected. Residual plots were explored for
261 violations of normality, and homoscedasticity and data were natural log-transformed when
262 necessary. The level of significance was set at $\alpha = 0.05$, and the analysis was performed in R
263 version 4.0.2 using the following packages: lme4 and eemans [48-50]. For descriptive and
264 inferential statistics, a value of one-half the detection (0.05 wt %) was applied to elements below
265 the detection limit [46, 51].

266

267 **3. Results**

268 For ten dolphins, age estimates ranged between 4.5 to 18 years (Table 1).
269 Hypermineralization precluded precise age estimates for two individuals; these individuals were
270 estimated to be >11 and >16 years old, respectively (Table 1). Tables 2 and 3 provide a summary
271 of the major, minor, and trace elements at each point measurement for all dolphins combined.
272 Data pertaining to each individual dolphin, including the mean and SE calculations, for each
273 point measurement are provided in Supplementary Tables 1-6.

274 Using SEM-EDS, we first compared the distribution of elements across the enamel and
275 pre-natal dentin. The mean \pm SE wt % for all point measurements and dolphins combined, were
276 as follows: O (39.6 ± 0.373), Ca (25.0 ± 0.229), P (14.6 ± 0.091), C (10.4 ± 0.287), Al ($8.29 \pm$
277 0.507), Mg (1.39 ± 0.070), Na (0.639 ± 0.013), and Cl (0.130 ± 0.007). For all elements, there
278 were significant differences in wt % values among the five points in the enamel and pre-natal
279 dentin (Table 2; Figure 3). For all models except for Mg, the random intercept model fit the data

280 better than the random intercept and slope model. Oxygen, Ca, and P were measured in lower wt
281 % values in the outer enamel (point 1) compared to the other points (points 2-5). Aluminum was
282 measured in the highest wt % in the outer enamel (point 1) and progressively decreased toward
283 the inner pre-natal dentin (Figure 3 and 4). For C, wt % values were higher in the outer enamel
284 and inner pre-natal dentin compared to points in the inner and mid enamel. The wt % of Mg was
285 lowest in the outer enamel and increased towards the inner pre-natal dentin. On average, the wt
286 % values of Mg were 2.21 and 0.84 in the enamel (points 1, 2, and 3) and pre-natal dentin (points
287 4 and 5), respectively. Sodium increased from the outer enamel to the EDJ and then decreased in
288 the inner pre-natal dentin; on average, the wt % values of Na in the enamel and pre-natal dentin
289 were 0.593 and 0.703, respectively. Finally, Cl was present in the greatest wt % in the outer
290 enamel (point 1); while Cl was also detected at lower wt % values in the mid-enamel and
291 innerenamel, it was not observed in the pre-natal dentin (points four and five). Elemental maps
292 showed differences in the distribution of elements between the enamel and pre-natal dentin
293 (Figure 4).

294 In the second analysis using SEM-EDS, we performed point analyses at seven points
295 approximating where GLG's would occur; a summary of the major, minor, and trace elements at
296 each point measurement for all dolphins combined is shown in Table 3. The mean \pm SE wt % for
297 all point measurements and dolphins combined, were as follows: O (41.6 ± 0.295), Ca ($23.8 \pm$
298 0.260), C (16.9 ± 0.608), P (13.5 ± 0.141), Mg (2.24 ± 0.053) Al (1.43 ± 0.215), and Na (0.698
299 ± 0.011) (Figure 5). For all elements, the intercepts model was a better fit than the intercepts and
300 slope model. Except for O, there were significant differences in the wt % values of the elements
301 across the seven points. The most common difference was between the tooth edge (point 1) and
302 the interior points (points 2-7). At the tooth edge (point 1), Ca, P, Mg, and Na were measured in

303 lower wt % values than the interior points (points 2-7). In contrast, C and Al were present at
304 higher wt % values closest to the in tooth edge (point 1) than in the interior points (points 2-7).
305 Visually the only differences that could be determined in the elemental maps were between the
306 dentin and pulp cavity (Figure 6).

307

308 **4. Discussion**

309 Using SEM-EDS, we were able to visualize the microstructure of dolphin teeth,
310 distinguishing between the enamel and dentin in the tooth crown, and explore the variation in
311 major (C, Ca, O, and P) and minor elements (Cl, Mg, Na) between the enamel and dentin. Except
312 for Al, no trace elements were detected. Although we could not visually distinguish GLG's based
313 on the SEM-EDS, we made use of images from tooth sections used the aging to approximate the
314 location where GLG's occurred and performed EDS analysis to investigate the potential
315 variation in major, minor, and trace elements across the GLG's. Except for the point closest to
316 the edge of the tooth, the wt % values of C, Ca, P, O, Mg, and Na did not vary substantially
317 across the dentin transect. Except for Al, we did not observe any other trace elements; therefore,
318 we could not examine how contaminants changed over time within the lifespan of an individual
319 or temporally across the decades among individuals. While technologies with lower detection
320 limits (e.g., LA-ICP-MS) may be required to explore the presence and distribution of trace
321 elements in bottlenose dolphin teeth, the information provided in the current study will be
322 valuable to other analyses such as LA-ICP-MS that rely on an Ca as an internal standard [10-
323 12,52]. Further, for some elements reported in this study (e.g., O, P, C, and Cl), it is either not

324 possible or very challenging to analyze using LA-ICP-MS; therefore, SEM-EDS can serve as a
325 complementary analysis [53].

326 The major elements detected in the dolphin teeth were C, Ca, P, and O. Calcium and P are
327 the primary components of hydroxyapatite; across all samples, the mean \pm SE wt % of C and P
328 was 24.2 ± 0.228 and 14.6 ± 0.091 , respectively. Murphy et al. [37] reported similar wt % values
329 for Ca (24.9) and P (11.2) in bottlenose dolphin dentin, also measured by SEM-EDS. However,
330 our values were lower than those reported by Loch et al. [19]; in analyzing the elemental
331 distribution in the enamel and dentin from ten dolphin species using WDX, Loch et al. [19]
332 reported wt % values of 46.9 and 36.2 for Ca and P, respectively for the single bottlenose
333 dolphin tooth analyzed. Unlike Loch et al. [19] and Brüggmann et al. [31], which reported the
334 element concentrations in the enamel and dentin of hippopotamid teeth, we did not determine
335 that Ca or P were consistently present in greater wt % values in the enamel compared to the
336 dentin. Brüggmann et al. [31] explain that the higher concentration of Ca and P in the enamel is a
337 result of the reduced porosity and increased mineralization of the enamel compared to the dentin.
338 Since the dentin has a higher percentage of organic components than enamel, when comparing
339 the enamel and dentin, we expected to find a higher weight percentage of the O and C in the
340 dentin, which are common elements found in proteins [26]. Oxygen followed this general
341 pattern, but C did not. Other major elements of proteins (e.g., collagens), such as nitrogen (N)
342 and hydrogen (H), were not detected. Hydrogen is too light to be detected using SEM-EDS, and
343 N generally produces too weak of a signal to be detected [26]. In the GLG's analysis, an
344 additional concern arose regarding the point closest to the tooth edge. In BSE mode, the
345 cementum was indistinguishable from the dentin; consequently, the points closest to the tooth
346 edge may have been cementum and not dentin. It is uncertain how wide the cementum layer was

347 in our samples; we also could not find an average cementum width in the literature for bottlenose
348 dolphins.

349 Overall, except for points analyzed closest to the tooth edge, the major elements (C, Ca, O,
350 and P) did not vary significantly across the tooth, making them good candidates for internal
351 standards in future LA-ICP-MS analyses. In contrast to SEM-EDS methodologies, which are
352 standardless, quantification in LA-ICP-MS involves external calibration using a standard
353 reference material (SRM) (e.g., NIST 612 glass or NIST 1486 bone meal for teeth samples). In
354 addition to external SRMs, signals are frequently normalized to an internal standard (e.g., Ca for
355 teeth), and studies often assume homogeneous distributions of the internal standard [53]. The
356 information provided here can help provide baseline information with respect to the wt % and
357 distribution of major elements in bottlenose dolphin teeth. The consistent distribution of major
358 elements across teeth supports their use as internal standards along with external CRMs.

359 The EDJ is a transition phase for major and minor elements. Cations and anions (e.g., Cl⁻,
360 Mg²⁺, and Na⁺) may also be incorporated into the hydroxyapatite structure of the enamel or
361 dentin during the pre-eruptive period [32]. In the case of the enamel, they may also be
362 incorporated post-eruption on the surface of the enamel (up to 150 μm depth) from the
363 surrounding saliva [55-56]. In the present study, we observed the same trends in the variation of
364 Cl and Mg across the enamel and pre-natal dentin as was previously reported in dolphin [19],
365 hippopotamus [31], and human teeth [26]. Chlorine decreased from the enamel towards the
366 dentin, while Mg increased from the enamel towards the dentin. Although the trends were not
367 consistent across individual dolphins, on average, we found that Na followed a similar
368 "umbrella" trend as was observed by Loch et al. [19], in which Na initially increased from the
369 outer enamel towards the inner enamel and then decreased moving further towards the inner

370 dentin. Throughout the secretory and maturation stages of enamel formation, elements enter the
371 enamel fluid; as the bioapatite crystallizes, the enamel becomes depleted in Mg and Na and
372 enriched in Cl. Therefore, Mg and Na are present in the greatest wt % near the EDJ, while Cl is
373 present in the greatest wt % in the outer enamel [31]. The incorporation of minor elements within
374 the tooth structure can alter the tooth function. More research is required to fully understand how
375 changes in minor elements alter the chemical structure and functionality of dental tissues.
376 However, previous studies focused on human, bovine, porcine, and ovine teeth have shown that
377 the incorporation of Mg^{2+} helps to regulate hydroxyapatite crystallization. For example, Mg is
378 present in higher concentrations in the dentin and the inhibition of crystallization may explain
379 why crystals are smaller and less frequently observed in the dentin compared to the enamel [26,
380 35].

381 During the mineralization phase of tooth development, trace elements can be
382 incorporated within the crystalline apatite [40, 56]. Previous studies have used trace element
383 concentration in marine mammal teeth to identify the timing of life-history events, identify the
384 maternal transfer of contaminants, explore habitat utilization, and assess the spatial and temporal
385 changes in environmental trace element concentrations, particularly those of anthropogenic
386 origin [10-12, 15, 58]. Except for Al, we did not observe trace elements [e.g., Cd, Cu, Hg, Pb,
387 Zn], which have been previously reported in marine mammal teeth [8-13, 15-17, 38-41]. Given
388 that Al decreased in wt % moving from tooth exterior towards the tooth interior, and Al is the
389 main component of the SEM stub, we suspect that the Al detected was related to the SEM stub
390 and not the tooth itself. Caceres-Saez et al. [42], measuring the major, minor, and trace elements
391 in Commerson's dolphin (*Cephalorhynchus c. commersonii*) and Franciscana dolphin
392 (*Pontoporia blainvillei*) bone samples using SEM-EDS also detected Al and came to a similar

393 conclusion. Our results indicate either 1) the abovementioned trace elements were not present in
394 our samples, or 2) they were present at concentrations below the detection limit. Based on the
395 findings of other studies, many trace elements that we expected to find (e.g., Cu, Cd, Hg, Zn) but
396 did not detect are likely present in the teeth but at wt %s below the detection limit of EDS
397 (approximately 0.1 wt%) [46].

398 Low sensitivity due to high elemental detection limits is a significant disadvantage of
399 using SEM-EDS technology to measure major, minor, and trace elements in dolphin teeth.
400 Detections can be optimized if the sample is properly prepared, and the scan parameters, such as
401 the vacuum conditions, accelerating voltage, spot size, and working distance are adjusted [26].
402 Ideally, the surface of the sample should be smooth and flat [54]. To minimize contamination,
403 we did not polish our samples; however, variation in the sample topography may have affected
404 the path of the x-rays exiting the surface and negatively influenced our ability to detect elements
405 [26,54]. Non-conductive samples are generally coated with carbon or gold-palladium (Au-Pd) to
406 reduce surface charging. After performing preliminary scans, we determined that there were no
407 issues with surface charging. Therefore, to avoid contamination, we did not coat the sample in
408 carbon or Au-Pd; however, the surface coating could have potentially increased the signal
409 strength and improved the signal-to-noise ratio [26]. Because teeth are non-homogenous
410 samples, it can be misleading to measure only one point, as some areas may have a greater
411 percentage of elements than others. We attempted to overcome this limitation by taking
412 measurements along several transects and averaging results. To maximize the detection of
413 characteristic x-rays, the accelerating voltage must be 2- to 3-times higher than the energy
414 required to eject an electron from its shell; in some cases, 20kv may not have been great enough
415 to optimize detections but using a higher voltage was not possible while working in low vacuum

416 mode, which is required for any samples that have not been dehydrated. Further, the working
417 distance, or the distance between the sample and the final piece of the lens, must be adjusted so
418 that the angle of the outgoing characteristic x-rays intersects the detection system. Finally, as
419 the mass percentage of the element decreases, the ability to correctly assign elemental peaks
420 decreases due to reduced counts of associated characteristic x-rays [54]. Although SEM-EDS has
421 several disadvantages, the technique provides a relatively quick method for elemental analysis;
422 in addition, when study methodologies do not require tooth sectioning, or utilize teeth that have
423 previously been sectioned, the method is non-destructive, making it appropriate for museum
424 specimens [40-42,46-467. To understand how trace element deposition in bottlenose dolphin
425 teeth may be used to create a timeline of life history events and exposure to trace elements,
426 particularly pollutants (e.g., Cd, Hg, Pb), additional research is required using technologies with
427 lower detection limits (e.g., LA-ICP-MS).

428

429 **References**

- 430 1. Myrick Jr, AC (1991) Some new and potential uses of dental layers in studying delphinid
431 populations. In: Pryor K, Norris, KS (eds) Dolphin societies: discoveries and puzzles.
432 University of California Press, Los Angeles, pp 251-279
- 433 2. Werth AJ (2000) Feeding in marine mammals. In: Schwenk K (ed) Feeding: form, function
434 and evolution in tetrapod vertebrates. Academic Press, San Diego, pp 487-526
- 435 3. Ungar P (2010) Mammal teeth: origin, evolution and diversity. The John Hopkins University
436 Press, Baltimore

- 437 4. Armfield BA, Zheng Z, Bajpai S, Vinyard CJ, Thewissen JGM (2013) Development and
438 evolution of the unique cetacean dentition. PeerJ 1:e24. <https://doi.org/10.7717/peerj.24>
- 439 5. Berta A, Sumich JL, Kovacs KM (2006) Diet, foraging, structures and
440 strategies. In: Berta A, Sumich JL, Kovacs KM (eds) Marine mammals: evolutionary
441 biology, 2nd edition. Academic Press, Burlington, pp 312–355
- 442 6. Wang F, Li G, Wu Z, Fan Z, Yang M, Wu T, Wang J, Zhang C, Wang S (2019) Tracking
443 diphyodont development in miniature pigs in vitro and in vivo. Biol Open 8(2):bio037036.
444 <https://doi.org/10.1242/bio.037036>
- 445 7. Outridge PM, Veinott G, Evans RD (1995) Laser ablation ICP-MS analysis of incremental
446 biological structures: archives of trace-element accumulation. Env Rev 3(2):160-170.
447 <https://doi.org/10.1139/a95-007>
- 448 8. Evans RD, Richner P, Outridge PM (1995) Micro-spatial variations of heavy metals in the
449 teeth of walrus as determined by laser ablation ICP-MS: the potential for reconstructing a
450 history of metal exposure. Arch Environ Contam Toxicol 28(1):55-60.
451 <https://doi.org/10.1007/BF00213969>
- 452 9. Ando N, Isono T, Sakurai Y (2005) Trace elements in the teeth of Steller sea lions
453 (*Eumetopias jubatus*) from the North Pacific. Ecol Res 20(4):415-423.
454 <https://doi.org/10.1007/s11284-005-0037-x>
- 455 10. Clark CT, Horstmann L, Misarti N (2020a) Zinc concentrations in teeth of female walruses
456 reflect the onset of reproductive maturity. Conserv Physiol 8(1):coaa029.
457 <https://doi.org/10.1093/conphys/coaa029>

- 458 11. Clark CT, Horstmann L, Misarti N (2020b) Evaluating tooth strontium and barium as
459 indicators of weaning age in Pacific walruses. *Methods Ecol Evol* 11(12):1626-1638.
460 <https://doi.org/10.1111/2041-210X.13482>
- 461 12. Clark CT, Horstmann L, Misarti N (2021) Walrus teeth as biomonitors of trace elements in
462 Arctic marine ecosystems. *Sci Total Environ* 145500.
463 <https://doi.org/10.1016/j.scitotenv.2021.145500>
- 464 13. De María M, Szteren D, García-Alonso J, de Rezende CE, Gonçalves RA, Godoy JM,
465 Barboza FR (2021) Historic variation of trace elements in pinnipeds with spatially segregated
466 trophic habits reveals differences in exposure to pollution. *Sci Total Environ* 750:141296.
467 <https://doi.org/10.1016/j.scitotenv.2020.141296>
- 468 14. Wenthrup-Bryne E, Armstrong CA, Armstrong RS, Collins BM (1997) Fourier transform
469 Raman microscopic mapping of molecular components in human tooth. *L. Raman Spectrosc*
470 28(2-3):151-158. [https://doi.org/10.1002/\(SICI\)1097-4555\(199702\)28:2/3<151::AID-](https://doi.org/10.1002/(SICI)1097-4555(199702)28:2/3<151::AID-JRS71>3.0.CO;2-5)
471 [JRS71>3.0.CO;2-5](https://doi.org/10.1002/(SICI)1097-4555(199702)28:2/3<151::AID-JRS71>3.0.CO;2-5)
- 472 15. Botta S, Albuquerque C, Hohn AA, da Silva VMF, Santos MCDO, Meirelles C, Barbosa L,
473 Di Beneditto APM, Ramos, RMA, Bertozzi C, Cremer MJ, Franco-Trecu V, Miekeley N,
474 Secchi ER (2015) Ba/Ca ratios in teeth reveal habitat use patterns of dolphins. *Mar Ecol Prog*
475 *Ser* 521:249-263. <https://doi.org/10.3354/meps11158>
- 476 16. Zheng Y, Zhang Y, Tang W, Guo H, Zhu Y, Dong Z, Jiang H (2018) Preliminary in situ
477 teeth study of the narrow-ridged finless porpoises remains using microsynchrotron radiation
478 X-ray fluorescence and laser ablation inductively coupled plasma mass spectrometry. *XRay*
479 *Spectrom* 47(5):388-395. <https://doi.org/10.1002/xrs.2955>

- 480 17. Kinghorn A, Humphries MM, Outridge P, Chan HM (2008) Teeth as biomonitors of
481 selenium concentrations in tissues of beluga whales (*Delphinapterus leucas*). *Sci Total*
482 *Environ* 402(1):43-50. <https://doi.org/10.1016/j.scitotenv.2008.04.031>
- 483 18. Loch C, Swain MV, van Vuuren LJ, Kieser JA, Fordyce RE (2013) Mechanical properties of
484 dental tissues in dolphins (Cetacea: Delphinoidea and Inioidea). *Arch Oral Biol* 58(7):773-
485 779. <https://doi.org/10.1016/j.archoralbio.2012.12.003>
- 486 19. Loch C, Swain MV, Fraser SJ, Gordon KC, Kieser, JA, Fordyce, RE (2014) Elemental and
487 chemical characterization of dolphin enamel and dentine using X-ray and Raman
488 microanalyzes (Cetacea: Delphinoidea and Inioidea). *J Struct Biol* 185(1):58-68.
489 <https://doi.org/10.1016/j.jsb.2013.11.006>
- 490 20. Cuy JL, Mann AB, Livi KJ, Teaford MF, Weihs TP (2002) Nanoindentation mapping of
491 mechanical properties of human molar tooth enamel. *Arch Oral Biol* 47(4):281-291.
492 [https://doi.org/10.1016/S0003-9969\(02\)00006-7](https://doi.org/10.1016/S0003-9969(02)00006-7)
- 493 21. Myick AC, Hohn AA, Sloan, PA, Kimura M, Stanley DD (1983). Estimating age of spotted
494 and spinner dolphins (*Stenella attenuata* and *Stenella longirostris*) from teeth. NOAA
495 Technical Memorandum. Southwest Fisheries Science Center, National Marine Fisheries
496 Service. Report number NOAA-TM-NMFS-SWFC-30. La Jolla, California, pp 17
- 497 22. Hohn AA, Scott MD, Wells RS, Sweeny JC, Irvine AB (1989) Growth layers in teeth from
498 free-ranging, known-age bottlenose dolphins. *Mar Mamm Sci* 5:315-342.
499 <https://doi.org/10.1111/j.1748-7692.1989.tb00346.x>

- 500 23. Hohn AA (2009) Age estimations. In: Perrin WF, Wursig B, Thewissen JGM (eds)
501 Encyclopedia of marine mammals, 2nd edn. Academic Press, London, pp 11-17.
- 502 24. Bowen WD, Northridge S (2010) Morphometrics, age estimation, and growth. In: Boyd IL,
503 Bowen WD, Iverson SJ (eds) Marine mammal ecology and conservation: A handbook of
504 techniques. Oxford University Press Inc., New York, pp 98-117
- 505 25. Vallet-Regí M, Navarrete DA (2016) Biological apatites in bone and teeth. In: Vallet-Regí
506 M, Navarrete DA (eds) Clinical use: from materials to applications. The Royal Society of
507 Chemistry, Cambridge, pp 1-29
- 508 26. Wang R, Zhao D, Wang Y (2020) Characterization of elemental distribution across human
509 dentin-enamel junction by scanning electron microscopy with energy-dispersive X-ray
510 spectroscopy. *Microsc Res Tech* <https://doi.org/10.1002/jemt.23648>
- 511 27. Simmer JP, Fincham AG (1995) Molecular mechanisms of dental enamel formation. *Crit*
512 *Rev Oral Biol Med* 6(2):84-108. <https://doi.org/10.1177/10454411950060020701>
- 513 28. Duckworth RM (2006) The teeth and their environment: Physical, chemical and biochemical
514 influences. Karger Publishers, Basel, Switzerland.
- 515 29. Goldberg M, Kulkarni AB, Young M, Boskey, A (2011) Dentin: structure, composition and
516 mineralization: The role of dentin ECM in dentin formation and mineralization. *Front Biosci*
517 (Elite Ed) 3:711-735. <https://doi.org/10.2741/e281>
- 518 30. Kang D, Amarasiriwardena D, Goodman AH (2004) Application of laser ablation–
519 inductively coupled plasma-mass spectrometry (LA–ICP–MS) to investigate trace metal

- 520 spatial distributions in human tooth enamel and dentine growth layers and pulp. *Anal Bioanal*
521 *Chem* 378:1608–1615. <https://doi.org/10.1007/s00216-004-2504-6>
- 522 31. Brüggmann G, Krause J, Brachert TC, Kullmer O, Schrenk F, Ssemmanda I, Mertz DF (2012)
523 Chemical composition of modern and fossil Hippopotamid teeth and implications for
524 paleoenvironmental reconstructions and enamel formation-Part 1: Major and minor element
525 variation. *Biogeosciences* 9(1):119-139. <https://doi.org/10.5194/bg-9-119-2012>
- 526 32. Curzon MEJ, Featherstone JDB (1983) Chemical composition in enamel. In: Lazari EP, Levy
527 BM (eds) *CRC handbook of experimental aspects of oral biochemistry*. CRC Press, Boca
528 Raton, FL, pp 123-135
- 529 33. Dorozhkin SV, Epple M (2002) Biological and medical significance of calcium phosphates.
530 *Angew Chem Int Ed* 41:3130-3146. [https://doi.org/10.1002/1521-](https://doi.org/10.1002/1521-3773(20020902)41:17<3130::AID-ANIE3130>3.0.CO;2-1)
531 [3773\(20020902\)41:17<3130::AID-ANIE3130>3.0.CO;2-1](https://doi.org/10.1002/1521-3773(20020902)41:17<3130::AID-ANIE3130>3.0.CO;2-1)
- 532 34. Rautray TR, Das S, Rautray AC (2010) In situ analysis of human teeth by external PIXE.
533 *Nucl Instrum Methods Phys Res B* 268(14):2371-2374.
534 <https://doi.org/10.1016/j.nimb.2010.01.004>
- 535 35. de Dios Teruel J, Alcolea A, Hernández A, Ruiz, AJO (2015) Comparison of chemical
536 composition of enamel and dentine in human, bovine, porcine and ovine teeth. *Arch Oral*
537 *Biol* 60(5):768-775. <https://doi.org/10.1016/j.archoralbio.2015.01.014>.
- 538 36. Yasukawa, A., Yokoyama, T., Kandori, K., Ishikawa, T. 2007. Reaction of calcium
539 hydroxyapatite with Cd²⁺ and Pb²⁺ ions. *Colloids and Surfaces A: Physicochemical and*
540 *Engineering Aspects*, 299(1-3), 203-208. <https://doi.org/10.1016/j.colsurfa.2006.11.042>

- 541 37. Stock SR, Finney LA, Telser A, Maxey E, Vogt S, Okasinski JS (2017) Cementum structure
542 in Beluga whale teeth. *Acta Biomater.* 48:289-299.
543 <https://doi.org/10.1016/j.actbio.2016.11.015>.
- 544 38. Murphy S, Perrott M, McVee J, Read FL, Stockin KA (2014) Deposition of growth layer
545 groups in dentine tissue of captive common dolphins (*Delphinus delphis*). *NAMMCO Sci.*
546 *Publ* 10:1-22. <https://doi.org/10.7557/3.3017>
- 547 39. Nganvongpanit K, Buddhachat K, Piboon P, Euppayo T, Kaewmong P, Cherdsukjai, P.,
548 Kittiwatanawong K, Thitaram, C (2017) Elemental classification of the tusks of dugong
549 (*Dugong dugong*) by HH-XRF analysis and comparison with other species. *Sci Rep* 7:46167.
550 <https://doi.org/10.1038/srep4616>
- 551 40. Ando-Mizobata N, Sakai M, Sakurai Y (2006) Trace-element analysis of Steller sea lion
552 (*Eumetopias jubatus*) teeth using a scanning X-ray analytical microscope. *Mamm Study*
553 31:65-68. [https://doi.org/10.3106/13486160\(2006\)31\[65:TAOSSL\]2.0.CO;2](https://doi.org/10.3106/13486160(2006)31[65:TAOSSL]2.0.CO;2)
- 554 41. Cruwys E, Robinson K, Davis NR (1994) Microprobe analysis of trace metals in seal teeth
555 from Svalbard, Greenland, and South Georgia. *Polar Rec* 30:49-52.
556 <https://doi.org/10.1017/S0032247400021057>
- 557 42. Cáceres-Saez I, Panebianco MV, Perez-Catán S, Dellabianca NA, Negri MF, Ayala CN,
558 Googall RNP, Cappozzo HL (2016) Mineral and essential element measurements in dolphin
559 bones using two analytical approaches. *Chem Ecol* 32(7):638-652.
560 <https://doi.org/10.1080/02757540.2016.1177517>

- 561 43. Sforza MC, Lugli F (2017) MapIT!: a simple and user-friendly MATLAB script to elaborate
562 elemental distribution images from LA-ICP-MS data. *J Anal At Spectrom* 32(5):1035-1043.
563 <https://doi.org/10.1039/C7JA00023E>
- 564 44. Ellingham ST, Thompson TJ, Islam M (2018) Scanning electron microscopy–energy-
565 dispersive X-ray (SEM/EDX): a rapid diagnostic tool to aid the identification of burnt bone
566 and contested cremains. *J Forensic Sci* 63(2):504-510. [https://doi.org/10.1111/1556-](https://doi.org/10.1111/1556-4029.13541)
567 [4029.13541](https://doi.org/10.1111/1556-4029.13541)
- 568 45. McCormack MA, Fattaglia F, McFee W, Dutton J (2020) Mercury concentrations in
569 blubber and skin from stranded dolphins (*Tursiops truncatus*) along the Florida and
570 Louisiana coasts (Gulf of Mexico, USA) in relation to biological variables. *Environ Res*
571 180:108886. <https://doi.org/10.1016/j.envres.2019.108886>.
- 572 46. Nasrazadani S, Hassani S (2016) Modern analytical techniques in failure analysis of
573 aerospace, chemical, and oil and gas industries. In: Makhlouf ASH, Aliofkhazraei M (eds)
574 Handbook of materials failure analysis with case studies from the oil and gas industry.
575 Elsevier, Oxford, UK, pp 39–54
- 576 47. Wolfgang WJ (2016) Chapter 14 - Chemical analysis techniques for failure analysis: Part 1,
577 common instrumental methods. In: Makhlouf ASH, Aliofkhazraei M (eds), Handbook of
578 material failure analysis with case studies from the aerospace and automotive industries,
579 Elsevier, pp. 279-307
- 580 48. R Core Team (2020) R: A language and environment for statistical computing. R
581 Foundation for Statistical Computing, Vienna, Austria. <https://www.R-project.org/>.

- 582 49. Bates D, Maechler M, Bolker B, Walker S (2015) Fitting Linear Mixed-Effects Models
583 Using lme4. J Stat Softw 67:1-48. <https://doi.org/10.18637/jss.v067.i01>
- 584 50. Length, R (2020) emmeans: Estimated Marginal Means, aka Least-Squares Means. R
585 package version 1.5.0. <https://CRAN.R-project.org/package=emmeans>
- 586 51. Adams DH, Engel ME (2014) Mercury, lead, and cadmium in blue crabs, *Callinectes*
587 *sapidus*, from the Atlantic coast of Florida, USA: a multipredator approach. Ecotoxicol
588 Environ Saf 102:196-201. <https://doi.org/10.1016/j.ecoenv.2013.11.029>
- 589 52. Limbeck A, Galler P, Bonta M, Bauer G, Nischkauer W, Vanhaecke F (2015) Recent
590 advances in quantitative LA-ICP-MS analysis: challenges and solutions in the life sciences
591 and environmental chemistry. Anal. Bioanal. Chem. 407(22):6593-6617.
592 <https://doi.org/10.1007/s00216-015-8858-0>
- 593 53. Perkin Elmer 2011. The 30-minute guide to ICP-MS.
594 [http://www.perkinelmer.com/CMSResources/Images/4474849tch_icpmsthirtyminuteguide.p](http://www.perkinelmer.com/CMSResources/Images/4474849tch_icpmsthirtyminuteguide.pdf)
595 [df.](http://www.perkinelmer.com/CMSResources/Images/4474849tch_icpmsthirtyminuteguide.pdf)
- 596 54. Newbury DE, Ritchie NWM (2013) Is scanning electron microscopy/energy dispersive X-ray
597 spectrometry (SEM/EDS) quantitative?. Scanning, 35(3), 141-168.
598 <https://doi.org/10.1002/sca.21041>
- 599 55. Lane DW, Peach DF (1997) Some observations on the trace element concentrations in human
600 dental enamel. Biol Elem Res 60:1-11. <https://doi.org/10.1007/BF02783305>

601 56. Reitznerová E, Amarasiriwardena D, Kopčáková M, Barnes RM (2000) Determination of
602 some trace elements in human tooth enamel. *Fresenius J Anal Chem* 367:748–754.
603 <https://doi.org/10.1007/s002160000461>

604 57. Driessens, FCM, Verbeeck RMH (1990) *Biomaterials*. CRC Press, Boca Raton, FL.

605 58. Outridge PM, Hobson KA, McNeely R, Dyke, A (2002) A comparison of modern and
606 preindustrial levels of mercury in the teeth of beluga in the Mackenzie Delta, Northwest
607 Territories, and walrus at Igloodik, Nunavut, Canada. *Arctic*. 55:123-132.

608

609

610

611

612

613

614

615

616

617

618

619

620 **Table 1** Stranding year, straight-line body length, sex, and estimated age of bottlenose dolphins
 621 used in the study

Sample ID	Stranding year	Length (cm)	Sex	Estimated age (years)
GA 159	1987	235	Female	>11 ^a
GA 260	1989	233	Female	8
GA 277	1989	245	Male	>16 ^a
GA 279	1989	244	Male	8
GA 345	1990	225	Female	4.5
GA 710	1995	238	Male	18
GA 737	1996	222	Male	8
GA 830	1996	237	Female	16
GA 1599	2009	221	Female	11
GA 1603	2009	241	Male	11
GA 1755	2012	224	Male	9
GA 1856	2014	226	Female	10

622 ^ahypermineralization near the pulp cavity precluded a more precise age estimate

Table 2 Weight percentage (wt %) of major, minor, and trace elements across the enamel and pre-natal dentin (PND) for all dolphins combined (mean \pm standard deviation; range of wt % in parenthesis) EDJ = enamel dentin junction

Element	Outer enamel Point 1	Mid-enamel Point 2	Inner enamel Point 3	PND near (EDJ) Point 4	Crown PND Point 5
<i>Major elements</i>					
C	11.6 \pm 6.40 (5.92 - 33.6)	8.69 \pm 2.28 (6.08 - 16.1)	9.30 \pm 2.84 (6.16 - 20.4)	10.2 \pm 2.21 (6.86 - 14.1)	12.0 \pm 2.48 (8.70 - 19.3)
Ca	23.7 \pm 4.91 (16.1 - 37.7)	25.7 \pm 3.19 (19.2 - 36.3)	25.5 \pm 2.03 (21.5 - 29.4)	25.0 \pm 1.73 (22.1 - 27.8)	26.0 \pm 1.74 (21.8 - 28.0)
O	34.1 \pm 5.80 (20.5 - 44.2)	38.9 \pm 5.02 (25.4 - 47.3)	41.4 \pm 3.05 (32.5 - 46.4)	41.7 \pm 2.53 (36.9 - 46.1)	41.5 \pm 2.56 (33.4 - 45.4)
P	13.44 \pm 1.83 (9.50 - 16.6)	15.0 \pm 0.939 (12.7 - 17.1)	15.1 \pm 0.803 (13.1 - 16.4)	14.8 \pm 0.737 (13.1 - 15.8)	14.8 \pm 0.504 (14.0 - 15.8)
<i>Minor elements</i>					
Cl	0.238 \pm 0.057 (0.110 - 0.390)	0.208 \pm 0.042 (0.130 - 0.340)	0.106 \pm 0.050 (0.050 - 0.170)	0.053 \pm 0.011 (0.050 - 0.100)	0.050 \pm 0.00 (0.050 - 0.050)
Na	0.477 \pm 0.153 (0.230 - 1.06)	0.598 \pm 0.110 (0.400 - 0.840)	0.705 \pm 0.108 (0.540 - 0.980)	0.742 \pm 0.162 (0.570 - 1.21)	0.668 \pm 0.174 (0.550 - 1.39)
Mg	0.298 \pm 0.394 (0.050 - 1.06)	0.734 \pm 0.623 (0.050 - 1.80)	1.42 \pm 0.414 (0.050 - 2.07)	1.86 \pm 0.362 (1.27 - 2.70)	2.57 \pm 0.384 (1.77 - 3.40)
<i>Trace elements</i>					
Al	16.2 \pm 8.45 (0.83 - 30.67)	9.80 \pm 5.65 (0.480 - 20.1)	6.50 \pm 3.80 (0.460 - 13.3)	5.79 \pm 3.35 (0.420 - 11.1)	3.52 \pm 1.67 (0.360 - 6.54)

Table 3 Weight percentage (wt %) of major, minor, and trace elements at seven points approximating where growth layers groups (GLG's) would occur in the dentin moving from point 1 (edge of tooth) towards the pulp cavity for all dolphins combined (mean \pm standard deviation; range of wt % in parenthesis)

Element	Point 1	Point 2	Point 3	Point 4	Point 5	Point 6	Point 7
<i>Major elements</i>							
C	34.7 \pm 17.1 (15.3 - 74.6)	17.24 \pm 1.85 (13.67 - 23.0)	14.5 \pm 1.64 (11.8 - 20.5)	13.5 \pm 1.52 (10.9 - 19.2)	14.2 \pm 3.52 (11.0 - 30.2)	13.0 \pm 1.72 (10.3 - 20.3)	12.9 \pm 2.22 (9.82 - 23.4)
Ca	16.58 \pm 6.44 (2.23 - 23.3)	23.5 \pm 1.59 (19.2 - 26.4)	24.8 \pm 2.16 (21.0 - 30.8)	25.3 \pm 1.75 (23.1 - 31.0)	24.80 \pm 2.05 (19.7 - 28.6)	26.2 \pm 2.25 (23.3 - 31.6)	25.2 \pm 1.10 (21.4 - 27.7)
O	33.7 \pm 7.00 (20.1 - 44.53)	41.5 \pm 3.01 (34.4 - 47.3)	42.6 \pm 2.66 (35.8 - 46.5)	43.2 \pm 2.19 (37.4 - 46.5)	43.34 \pm 2.42 (33.7 - 48.9)	42.3 \pm 3.07 (34.9 - 46.1)	43.8 \pm 1.73 (38.1 - 45.8)
P	9.33 \pm 3.60 (1.27 - 12.8)	13.2 \pm 0.681 (11.8 - 15.0)	14.0 \pm 0.703 (12.0 - 15.4)	14.4 \pm 0.543 (13.5 - 15.8)	14.2 \pm 1.02 (11.4 - 15.4)	14.8 \pm 0.532 (13.7 - 16.1)	14.51 \pm 0.492 (12.5 - 15.4)
<i>Minor elements</i>							
Mg	0.818 \pm 0.698 (0.050 - 2.29)	2.06 \pm 0.484 (1.32 - 2.88)	2.37 \pm 0.664 (0.005 - 3.67)	2.55 \pm 0.608 (1.85 - 4.05)	2.57 \pm 0.639 (1.73 - 4.19)	2.62 \pm 0.661 (1.00 - 3.90)	2.60 \pm 0.421 (1.96 - 3.56)
Na	0.501 \pm 0.276 (0.050 - 1.06)	0.667 \pm 0.109 (0.540 - 1.01)	0.711 \pm 0.148 (0.520 - 1.22)	0.724 \pm 0.122 (0.540 - 1.03)	0.719 \pm 0.134 (0.480 - 1.08)	0.709 \pm 0.113 (0.550 - 1.03)	0.748 \pm 0.099 (0.600 - 0.980)
<i>Trace elements</i>							
Al	4.97 \pm 7.54 (0.050 - 23.80)	1.84 \pm 2.68 (0.050 - 8.47)	1.14 \pm 1.63 (0.050 - 6.25)	0.777 \pm 1.20 (0.050 - 4.84)	0.654 \pm 1.14 (0.050 - 4.53)	0.506 \pm 1.02 (0.050 - 4.32)	0.404 \pm 0.913 (0.050 - 3.81)

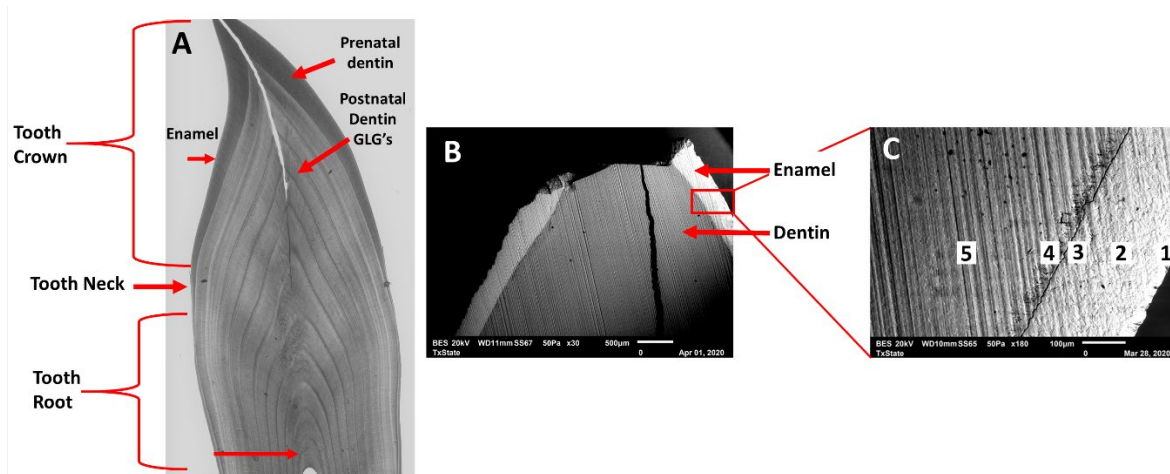


Figure 1 Cross-sectioned image of the top half of tooth of GA1603 (the split in the tooth was likely a result of being frozen in long-term storage; arrows represent the general location of the elemental analyses) (A), SEM backscattered imaging showing (B) the enamel and pre-natal dentin (PND), along with a rectangle that indicates the approximate area of SEM-EDS analysis, and (C) a zoomed in image of the area of the EDS analysis showing the locations for point analysis (point 1 = outer enamel, point 2 = mid enamel, point 3 = inner enamel, point 4 = pre-natal dentin near the enamel pre-natal dentin junction, and point 5 = inner pre-natal dentin)

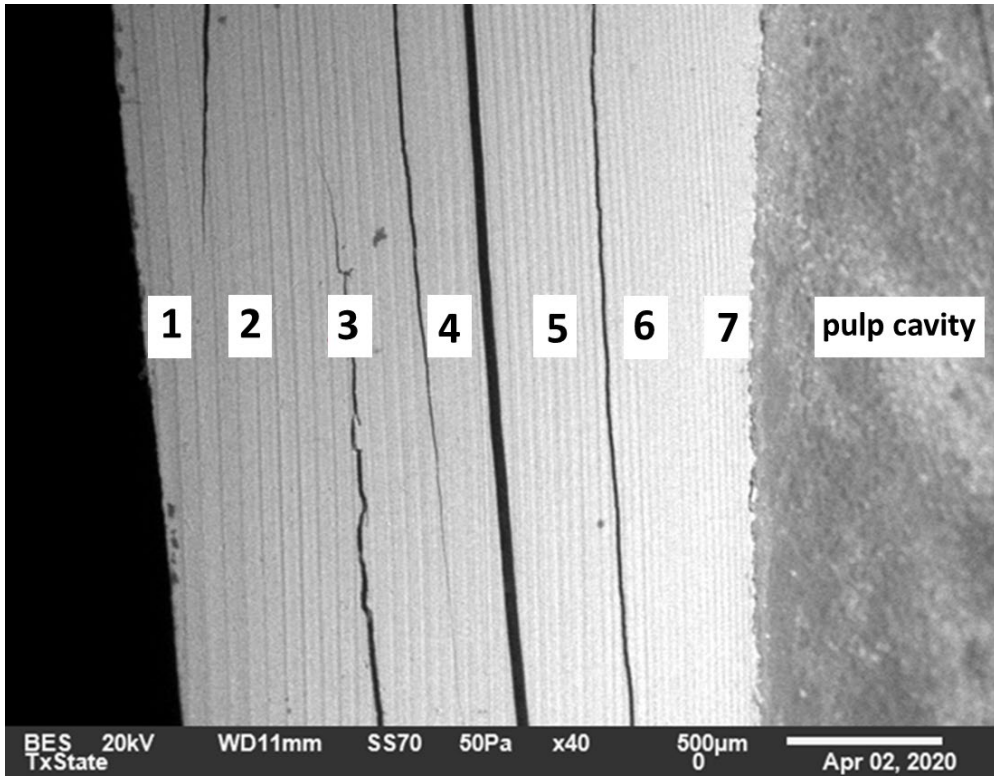


Figure 2 SEM backscattered image showing the locations of point analyses (points 1 - 7) used to explore the distribution of elements across the approximate location of the growth layer groups (GLG's).

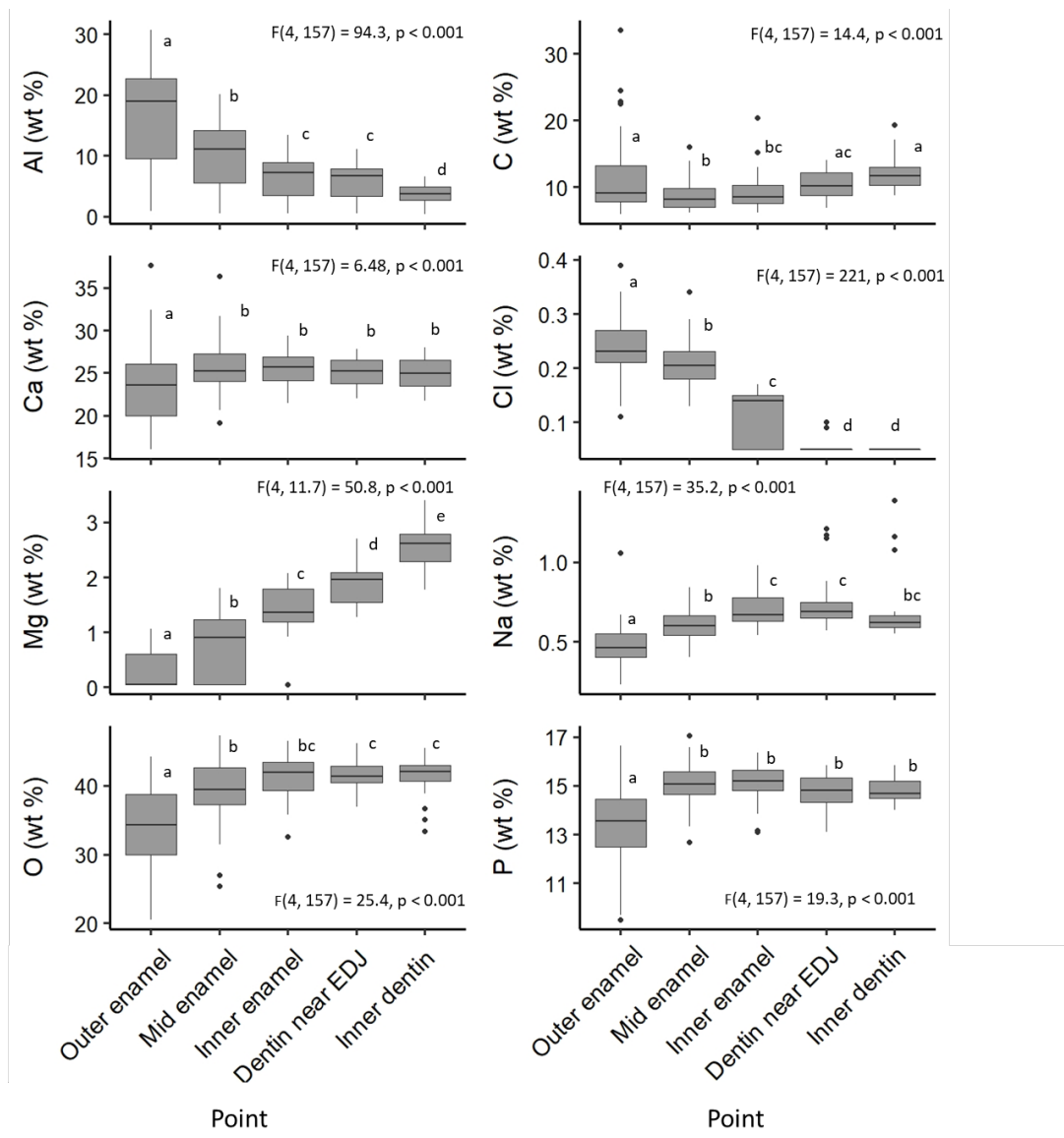


Figure 3 Selective point analyses for elements in the enamel and pre-natal dentin (PND) expressed as weight percentage (wt %): outer enamel (point 1), mid enamel (point 2), inner enamel (point 3), pre-natal dentin near enamel dentin junction (EDJ) (point 4), inner pre-natal dentin (point 5). Results of the repeated-measures linear mixed effects ANOVA and Tukey's post-hoc test are shown in each panel. Lowercase letters indicate points grouped by statistically similar wt % values. Data pertaining to each individual dolphin including the mean and SE wt % at each point are provided in the supplementary tables S1-S3.

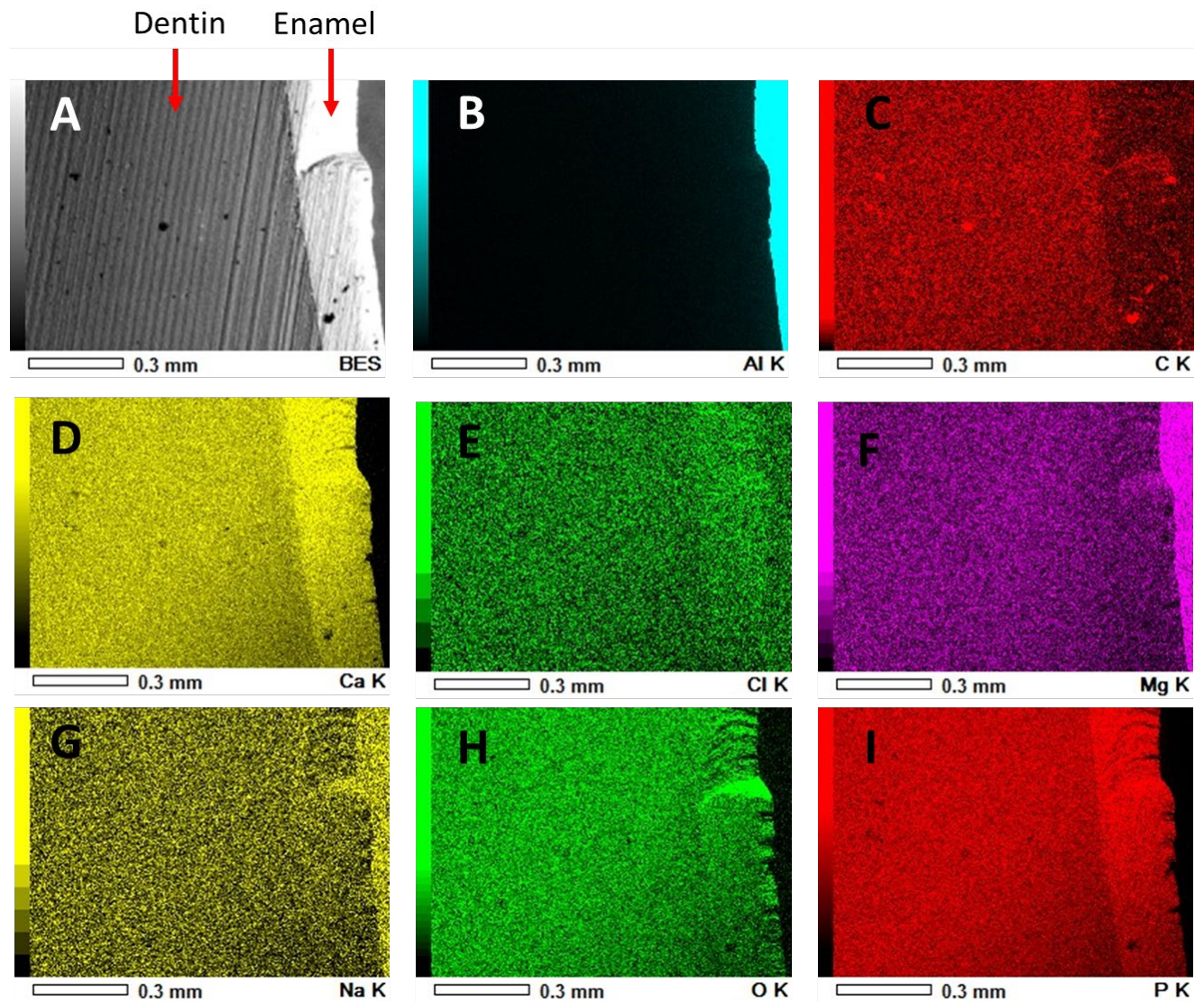


Figure 4 Backscatter SEM image of analysis area of sample GA 260 showing the enamel and pre-natal dentin (PND) (panel A) and elemental maps for Al (panel B), C (panel C), Ca (panel D), Cl (panel E), Mg (panel F), Na (panel G), O (panel H), and P (panel I). The intensity of the color is proportional to the number of x-ray counts in which higher intensity colors correspond to higher x-ray counts or greater wt %. For references to color please refer to the online version of this article

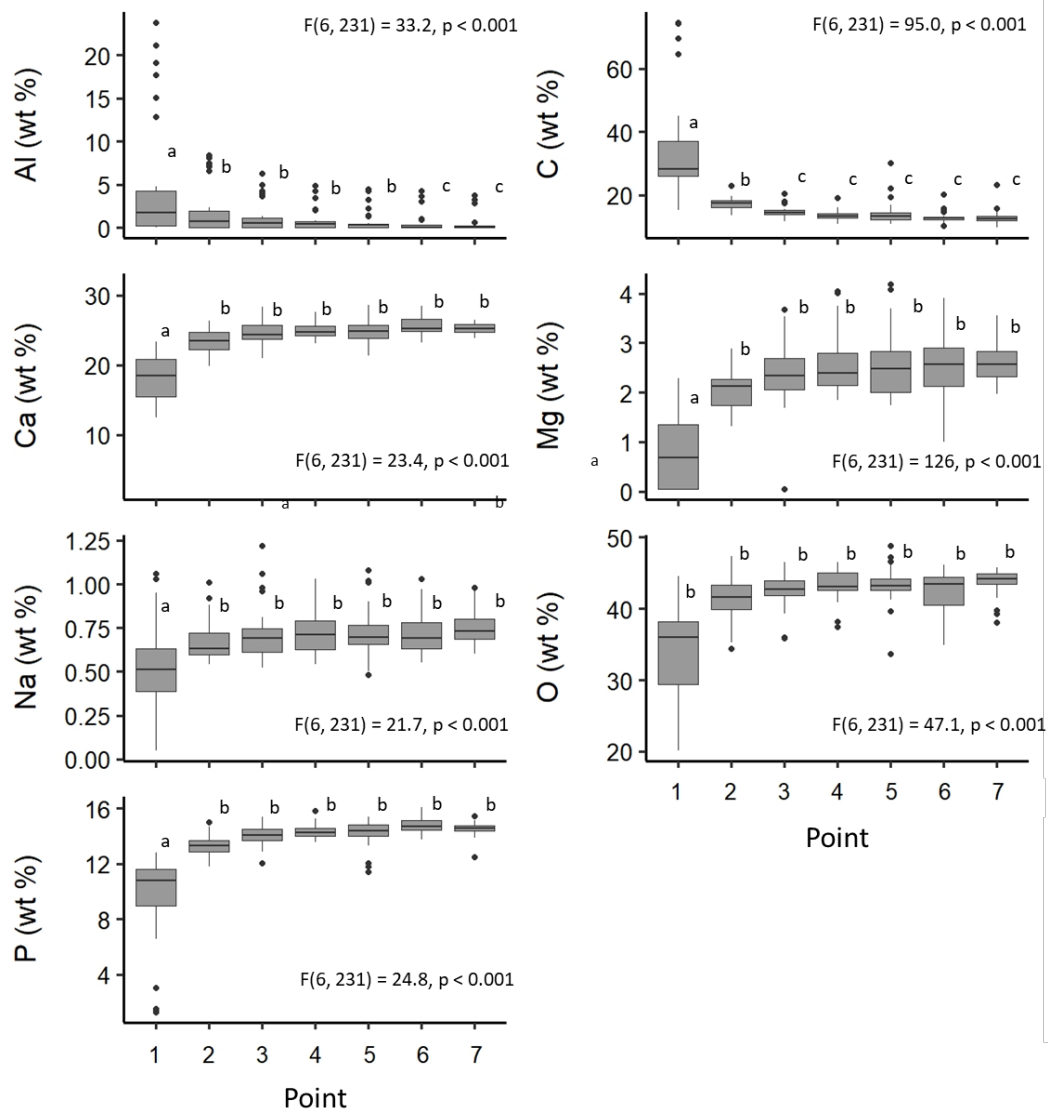


Figure 5 Selective point analyses for elements approximating where growth layers groups (GLG's) are present. Elements presented as a weight percentage (wt %), moving from the outer tooth edge (point 1) towards the tooth center (point 7), with points closest to the tooth edge being the oldest deposited dentin layers and points closest to the tooth center being the newest deposited dentin layers. Results of the repeated-measures linear mixed effects ANOVA and Tukey post-hoc test are shown in each panel. Pairwise comparisons for Al are not included

because the confidence intervals of the marginal means included zero. Lowercase letters indicate points grouped by statistically similar wt % values. Data pertaining to each individual dolphin including the mean and SE wt % at each point are provided in the supplementary tables S4-S5.

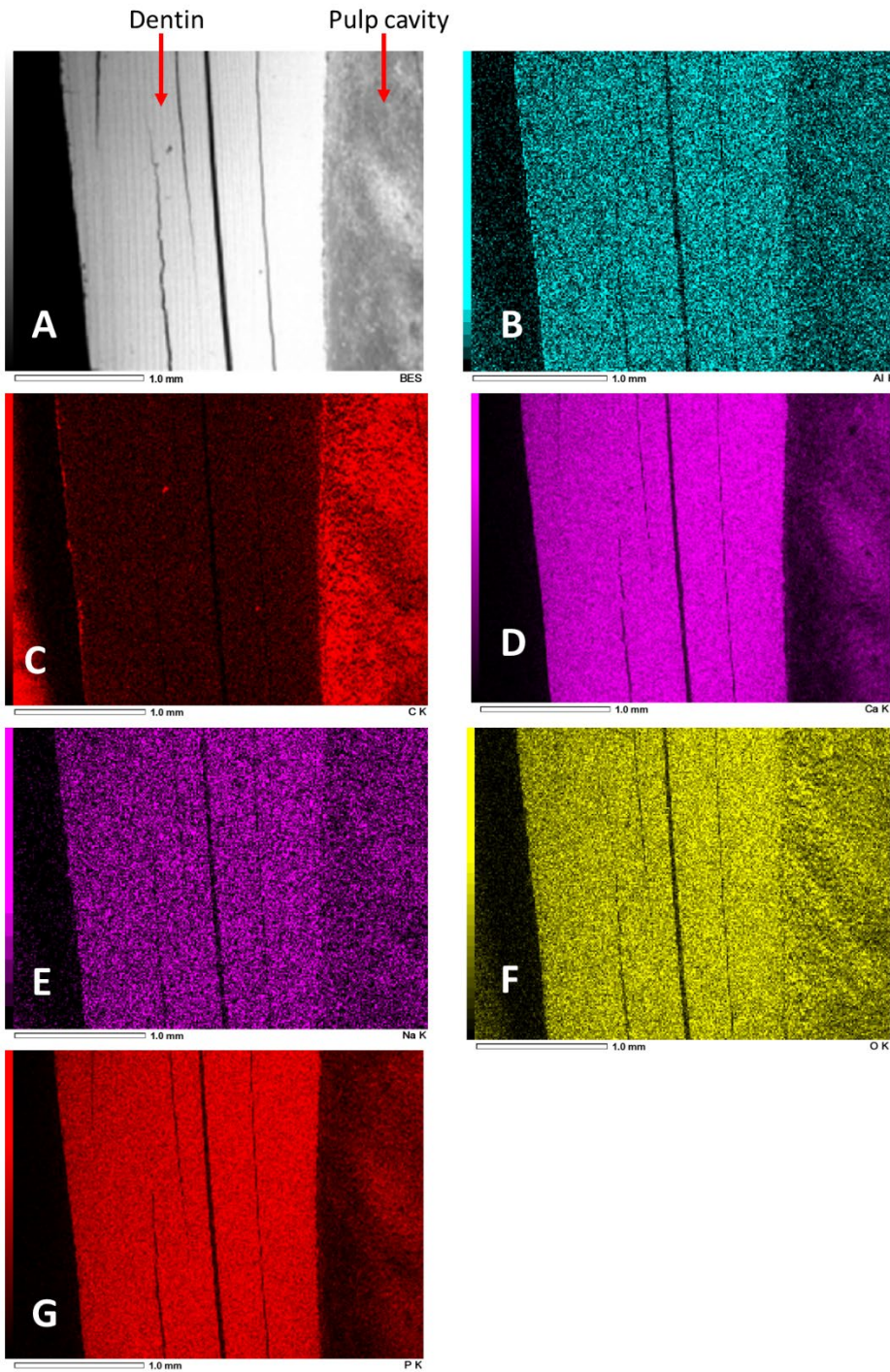


Figure 6 Backscatter SEM image of analysis area of sample GA 1755 showing the dentin and pulp cavity (panel A) and elemental maps for Al (panel B), C (panel C), Ca (panel D), Na (panel

E), O (panel F), and P (panel G). Magnesium and Cl were not detected in this particular sample. The intensity of the color is proportional to the number of x-ray counts in which higher intensity colors correspond to higher x-ray counts or greater wt %. Striations in the tooth may be a consequence of the cross-sectioning process. For references to color please refer to the online version of this article.